HHS Public Access

Author manuscript

*Ultrasound Med Biol*. Author manuscript; available in PMC 2018 January 10.

Published in final edited form as:

*Ultrasound Med Biol*. 2017 January ; 43(1): 91–103. doi:10.1016/j.ultrasmedbio.2016.08.021.

# Using speed of sound imaging to characterize breast density

**Mark Sak**[1], **Neb Duric**[1], **Peter Littrup**[1,2], **Lisa Bey-Knight**[3], **Haythem Ali**[4], **Patricia Vallieres**[4], **Mark E. Sherman**[5], and **Gretchen L. Gierach**[6]

[1]Delphinus Medical Technologies, 46701 Commerce Center Dr, Plymouth, MI, 48170 [2]Brown University, Rhode Island Hospital, 593 Eddy Street, Providence RI, 02903 [3]Karmanos Cancer Institute, Wayne State University, 4100 John R Street, Detroit MI 48201 [4]Henry Ford Health System, 2799 W Grand Boulevard, Detroit MI 48202 [5]Division of Cancer Prevention, National Cancer Institute, Department of Health and Human Services, 9609 Medical Center Dr. MSC 9774, Bethesda, Maryland 20892 [6]Metabolic Epidemiology Branch, Division of Cancer Epidemiology and Genetics, National Cancer Institute, 9609 Medical Center Dr. MSC 9774, Bethesda, Maryland 20892

## Abstract

A population of 165 women with negative mammographic screens also received an ultrasound tomography (UST) exam at the Karmanos Cancer Institute (KCI) in Detroit, MI. Standard statistical techniques were employed to measure the associations between the various mammographic and UST related density measures and various participant characteristics such as age, weight and height. The Mammographic percent density (MPD) was found to have similar strength associations with UST mean sound speed (Spearman coefficient, $r_s = 0.722$, $p < 0.001$) and UST median sound speed ($r_s = 0.737$, $p < 0.001$). Both were stronger than the associations between MPD with two separate measures of UST percent density, a k-means ($r_s = 0.568$, $p < 0.001$) or a threshold ($r_s = 0.715$, $p < 0.001$) measure. Segmentation of the UST sound speed images into dense and non-dense volumes showed weak to moderate associations with the mammographically equivalent measures. Relationships were found to be inversely and weakly associated between age and the UST mean sound speed ($r_s = -0.239$, $p = 0.002$), UST median sound speed ($r_s = -0.226$, $p= 0.004$) and MPD ($r_s = -0.204$, $p= 0.008$). Relationships were found to be inversely and moderately associated between BMI and the UST mean sound speed ($r_s = -0.429$, $p < 0.001$), UST median sound speed ($r_s = -0.447$, $p < 0.001$) and MPD ($r_s = -0.489$, $p < 0.001$). The results confirm and strengthen findings presented in previous work indicating that UST sound speed imaging yields viable markers of breast density in a manner consistent with

**Address for correspondence:** Mark Sak, Delphinus Medical Technologies, 45525 Grand River Avenue, Novi, MI, 48374, msak@delphinusmt.com.



**Conflicts of Interest**

Neb Duric and Peter Littrup have financial interests in Delphinus Medical Technologies Inc. whose SoftVue scanner was used in this study. Financial conflicts of interest are being managed by Wayne State University. No other authors declare any financial conflicts of interest.

mammography, the current clinical standard. These results lay the groundwork for further studies to assess the role of sound speed imaging in risk prediction.

**Keywords**

Breast density; Ultrasound tomography; Mammography; Breast Cancer; Sound speed; Dense and non-dense breast volumes; risk assessment

## Introduction

Of the many factors that affect the risk of developing breast cancer, breast density has been shown to be one of the strongest. Numerous epidemiologic studies conducted over the past four decades have consistently demonstrated that increased mammographic density is related to increased breast cancer risk (Huo, et al. 2014, McCormack and dos Santos Silva 2006, Pettersson, et al. 2014, Sak, et al. 2015). It was determined that, when compared to women with lower densities, women with the highest mammographic densities showed a 4 to 6-fold increased risk of breast cancer.

Breast density generally refers to the amount of dense tissue visible on a mammographic image. Dense breast tissue attenuates more x-rays than non-dense tissue and therefore appears radiopaque on a mammogram. Measuring breast density is ultimately a measure of the amount of white regions in the image and can be done both qualitatively and quantitatively. Mammographic percent density (MPD) is defined as the ratio of dense breast tissue relative to the total amount of breast tissue seen on a mammogram and is measured using computer-assisted programs such as Cumulus (Byng, et al. 1994) or can be measured volumetrically using programs such as Volpara (Eng, et al. 2014, Jeffreys, et al. 2010) and Quantra (Ciatto, et al. 2012, Regini, et al. 2014). However, despite being the current gold standard for breast imaging, mammography poses some shortcomings for the measurement of breast density (Kopans 2008, Sak, et al. 2015).

Ultrasound tomography (UST) is an emerging imaging modality that produces three-dimensional images of breast tissue (Duric, et al. 2005, Duric, et al. 2010). In UST, sound waves are used to measure the reflection and transmission properties of breast tissue (Li, et al. 2008). Physical breast density can be directly measured using UST by measuring the transmission property known as sound speed. Ignoring shear waves, the sound speed of any material is given by $v = (C/\rho)^{1/2}$ where C is the bulk modulus and $\rho$ is the density of the material in question. Studies have shown that for breast tissues, the bulk modulus scales as the cube of density (Mast 2000, Masugata, et al. 1999, Weiwad, et al. 2000). Substituting this into the equation for sound speed removes the dependence on bulk modulus and leaves a direct relationship between tissue density and the measured tissue sound speed, ($v \propto \rho$). This direct relationship suggests that sound speed images may be a useful tool for directly measuring physical breast density and its distribution throughout the breast.

Previous work (Duric, et al. 2013, Sak, et al. 2012, Sak, et al. 2011, Sak 2013) has compared breast density measurements between mammographic percent density with volume averaged sound speed and shown that the two different imaging modalities correlate strongly with

each other. These results were accomplished using symptomatic participants that were not screened according to a standardized research protocol. The work presented here examines, for the first time, the 3-dimensional sound speed properties of the breast among healthy women who were screen negative on mammography.

## Methods

### Participant recruitment

The study described here is part of a larger ongoing observational study, the Ultrasound Study of Tamoxifen, aimed at measuring breast density changes among women aged 30–70 years undergoing treatment with tamoxifen (Sak, et al. 2013). Exclusion criteria included weight > 250 lbs, breast diameter > 20 cm (the maximum allowable for the scanner), pregnancy, breastfeeding, current breast implants and active breast skin infections. The study includes two groups: 1) women receiving tamoxifen for clinical indications and 2) a comparison group of screen negative women frequency matched on age, race and menopausal status. The main aim of the Ultrasound Study of Tamoxifen is to evaluate changes in breast density as measured using both mammography and UST 12 months after a baseline scan for both groups. The analysis presented herein involves only the baseline UST scans and mammograms that became available for the comparison group of 165 women with negative mammographic screens.

To be eligible for the comparison group, a screening mammogram must first be identified with the recommendation to continue routine screening. Any potential participant would then be age-, race-, and menopausal status-matched to the case group before then being offered a UST scan. There was therefore a short temporal delay between the scans. Digital mammograms were obtained at the Karmanos Cancer Institute (KCI) or at the nearby referring Henry Ford Hospital (HFH) in Detroit, Michigan. Both sites are certified by the American College of Radiology’s Mammography Accreditation Program and maintain image quality control according to the Mammography Quality Standards Act (MQSA). All UST scans were performed with a UST imaging device located at the Karmanos Cancer Institute. The scans were collected over a period of three years, ranging from 2011 to 2014. At the time of the UST scan, additional participant characteristics such as measured weight and height were also collected. All imaging procedures were performed under an Institutional Review Board-approved protocol, in compliance with the Health Insurance Portability and Accountability Act, with informed consent obtained from all patients.

### Mammographic image acquisition

Digital mammograms were obtained and analyzed for all 165 participants. Mammograms from KCI were obtained on a GE Senographe Essential digital mammography unit (General Electric Company, Fairfield Connecticut, USA) while participants imaged at HFH were imaged on a Hologic Lorad Selenia digital mammography unit (Hologic, Bedford Massachusetts, USA). One craniocaudal view of one breast for each participant was analyzed. All mammographic images were of diagnostic quality and were obtained with clinical image quality standards (e.g. exposure, pectoralis visualization, etc.). The breast that was chosen to be analyzed (left or right) was randomized. Mammographic percent density

was measured by one reader (NFB) using the CUMULUS 4 software (University of Toronto, Ontario, Canada) (Byng, et al. 1994). This interactive computer-assisted method was used to obtain measurements of the areas of dense tissue and total breast area on each mammogram in a similar manner to that reported in earlier work (Duric, et al. 2013, Sak, et al. 2012, Sak, et al. 2011, Sak 2013). From these measurements, the area of non-dense tissue and percent density (dense area divided by total breast area) was calculated. Reproducibility of the mammographic methods was assessed by rereading a randomly selected sample of images, randomly distributed among the images being read, within and between each reading session. In total, 17 participants had their mammographic density reread and an ICC of 0.71 for the percent density values was measured which indicates good reliability.

## UST image acquisition

Operation of the UST devices has been described previously (Duric, et al. 2013, Duric, et al. 2009, Duric, et al. 2007, Sak, et al. 2012, Sak, et al. 2011, Sak 2013). The participant lies prone on the device with their breast submerged in a water bath to act as an ultrasound coupler. The UST hardware creates tomographic sound speed images of the breast from the chest wall to the nipple. Sound speed and density information were extracted from the images using a semi-automated method in the software package ImageJ (US National Institutes of Health, Bethesda Maryland, USA) (Rasband 1997–2012) by one reader (M. Sak). There is a demonstrated reliability in sound speed estimates when processing UST scans in this manner, with a reported ICC of 0.934 for sound speed measurements (Khodr, et al. 2015). The sound speed of the surrounding water bath is intermediate to the sound speeds of the breast tissue and must therefore be segmented from each image manually. Also, the reader removed image slices that corresponded to the chest wall and the nipple as these regions are not relevant to breast density measurements. Over the course of the study, the UST hardware used to create UST sound speed images was upgraded. Initially, a clinical UST prototype known as the Computed Ultrasound Risk Evaluation (CURE) (Karmanos Cancer Institute, Detroit Michigan, USA) system was used (N=27)(Duric, et al. 2007). An upgraded version of the hardware known as SoftVue (Delphinus Medical Technologies, Plymouth, Michigan, USA) was installed early into the recruitment period (N=138)(Duric, et al. 2013, Sak, et al. 2014). Comparability of sound speed estimates generated by both devices was found to be excellent.

## UST image and statistical analysis

**Quantitative Volumetric Sound Speed—**Once manual segmentation of breast tissue from the water bath is complete, the sound speed of each voxel within a defined volume of breast tissue (1–3 cubic millimeters depending on slice thickness) is defined. The volume averaged sound speed (VASS) is the *mean* value of the sound speed of the manually defined breast tissue and was calculated for each participant. However, the distribution of sound speed within a single participant may be skewed (i.e. not normally distributed). The mean sound speed value may not be sensitive to these distributions and may not be the best measure of determining the average breast density. Novel techniques of using the volumetric *median* and *modal* sound speed values were therefore also calculated for each participant. The median sound speed was calculated by sorting an array containing the sound speed value of each voxel and selecting the value contained in the central position of the array. A

histogram of the distribution of the sound speed values was created for each participant with a range of 1300 m/s to 1600 m/s and divided into ImageJ's default setting of 256 bins. The modal sound speed corresponded to the bin with the greatest number of counts.

**Subregion Sound Speed—**UST breast density is measured fundamentally differently from mammographic density because of the quantitative nature of UST sound speed images, as noted above. This quantification also allows additional options for segmentation. An attempt to measure UST density in a manner similar to mammographic density was thereby performed by separating the UST sound speed images into volumes of dense and non-dense tissue. The measured volumes could be used to calculate a UST percent density value in a similar fashion to how MPD is calculated. In addition, the mean sound speed of each subregion was also calculated by measuring the mean voxel value for each subregion. These estimates are referred to as subregion density measures in this paper.

This segmentation of the UST sound speed images into dense and non-dense tissue was done in two different ways (Figure 1):

i. *K-means segmentation method* – A k-means clustering plugin for ImageJ was used to separate each sound speed image for each participant into dense and non-dense subregions (Jain and Dubes 1988).

ii. *Threshold segmentation method* – An operator-independent threshold of 1460 m/s was used to separate each image into dense and non-dense regions. Voxels that had a sound speed greater than or equal to 1460 m/s were classified as dense and voxels that had a sound speed less than 1460 m/s were classified as non-dense. After a brief initial review of the data, the threshold of 1460 m/s was determined to produce the widest possible range of percent density values. Setting a higher or lower threshold caused the measured percent density to be pushed towards 0% or 100% respectively and therefore limited the range of values.

## Results

### Characteristics of the study population

The cohort-averaged participant characteristics, UST and mammographic density measurements and UST subregion density measures are shown in Table 1. On average, participants were 51 years of age and their BMI was classified as obese (BMI = 31 kg/m$^2$). The average values for the mean (1450 m/s), median (1446 m/s) and modal (1440 m/s) sound speed and average MPD (22.4%) indicate that this population had low breast density which would be consistent with the measured age and BMI. Finally, because the participants were not enrolled into the study until after a negative screening mammogram was identified, the UST scan occurred an average of 42 days after the mammogram. These were otherwise healthy women that were not undergoing hormonal therapy, therefore, changes in the composition of glandular tissue between the mammographic and UST scans should be minimal. Changes in breast density modulated by hormonal changes during the menstrual cycle have also been shown to be minimal for UST sound speed measurements (Duric, et al. 2013). Fluctuations in weight between the scans could have affected breast density as could

the known association between increasing age and decreasing breast density. However, given the time frame of 42 days, both of these factors likely produced minimal, if any measured difference in the glandular tissue composition between modalities.

## Frequency distributions of average UST and mammographic density measures

Figure 2 shows the distribution of the mean, median and modal sound speed values over all participants. All three of these UST sound speed distributions are strongly peaked. Figure 3 shows the frequency distributions for the percent density measurements calculated using mammography and for both the UST k-means and thresholding clustering methods. The distribution of MPD is different from that of the UST sound speed values by being less peaked at lower values. Although most participants have low breast density irrespective of the imaging modality employed, the MPD distribution is more spread out over these smaller values. The k-means and threshold clustering methods produce similar UST percent density measurements (25.3% and 25.5% respectively), but the distribution of the measurements differs. The UST threshold percent density measure is peaked sharply towards lower values, resembling the distribution of UST sound speed in this study population. The distribution of the UST k-means clustering percent density values covers a smaller range (10% to 60% instead of 10% to 100%). This aligns more closely with other volumetric analysis of percent density, such as Quantra and Volpara, which tend to measure much lower percent density and a narrower range than Cumulus does (Ciatto, et al. 2012, Eng, et al. 2014, Jeffreys, et al. 2010, Regini, et al. 2014).

## Subregion frequency distributions

Figure 4, Figure 5 and Figure 6 show the frequency distributions for the dense, non-dense and total breast areas and volumes respectively, as calculated using mammography and UST. The dense (Figure 4) and non-dense (Figure 5) tissue measures have similar distributions for both mammography and the UST threshold method, but the k-means clustering method gives a slightly more peaked non-dense volume distribution. The whole breast area and volume measures (Figure 6) are similarly distributed between the 2D mammography and 3D UST modalities.

## Associations between UST and mammographic density measures

UST breast density measures were found to be strongly correlated with mammographic breast density measures. Plots demonstrating the positive correlations of mean, median and modal sound speed values with mammographic percent density are shown in Figure 7. Table 2 shows the measured Spearman correlation coefficients between MPD and mean, median and modal UST sound speed values with the various UST and mammographic subregion density measures. For most measures, the mean, median and modal sound speed show similar associations, both in strength and magnitude. The median and mean sound speed show almost identical correlations while the modal sound speed shows slightly weaker correlations. In particular, MPD shows positive correlations with median sound speed ($r_s$ = 0.737, $p < 0.001$) and mean sound speed ($r_s$ = 0.722, $p < 0.001$) that were slightly stronger than that observed with modal sound speed ($r_s$ = 0.651, $p < 0.001$). This indicates a strong relationship between 2D mammographic density measures and 3D UST density measures.

The UST and mammographic subregion measures were compared with each other using Spearman correlations. Table 3 shows the comparison of the two different UST segmentation methods and finds that dense volume, non-dense volume and UST percent density correlate strongly for the two segmentation methods. Table 4 compares the two UST subregion measures with the mammographic measures. Here, the correlations of both measures of dense volume with the mammographic dense area were weak to moderate ($r_s = 0.198$, $p = 0.011$ for k-means segmentation and $r_s = 0.466$, $p < 0.001$ for threshold segmentation). Although UST dense volume is assumed to be the three-dimensional equivalent of the mammographic dense area, differences in how each technique measures the same structures are evident in these results as the correlations do not always align strongly with each other.

### Associations with continuous participant characteristics

The continuous participant characteristics of age, height, weight and BMI were associated with average mammographic and UST density and subregion density measures. The results are shown in Table 5. In general, the correlations involving height were not statistically significant. The average UST and mammographic density measures were inversely related to the participant factors of age, weight and BMI with the associations involving weight and BMI being of moderate strength while those involving age being weaker. Both age and weight are known factors that affect MPD (Byrne, et al. 1995, Schetter, et al. 2014).

## Discussion

Elevated breast density is a strong risk factor for developing breast cancer, but developing the most clinically useful methods for measuring density is a topic of ongoing research. Herein we demonstrate that volumetric breast density measurements using sound speed correlate with mammographic density (the current clinical standard) in a relevant participant group – healthy women with negative mammographic screens for whom estimating risk might have relevance for guiding future screening and prevention procedures.

Previous work (Duric, et al. 2013, Sak, et al. 2012, Sak, et al. 2011, Sak 2013) that examined the relationship between MPD and UST sound speed was based on participants with abnormalities who were not representative of the general (healthy) population. Density measurements from that group may have been influenced by (i) the presence of high sound speed masses which contaminated the breast density measurements and (ii) characterisitics of a participant population that is not disease free and whose breast density may therefore differ from the general population. To address these potential concerns, we have performed the current analysis on a population of screen negative women, which confirms and extends the previous work (Duric, et al. 2013, Sak, et al. 2012, Sak, et al. 2011, Sak 2013) demonstrating strong, positive correlations between breast density measures obtained from UST sound speed imaging and digital mammography.

A similar strength of correlation between mean UST sound speed and MPD was observed as before ($r_s = 0.710$, $p < 0.001$) and in this work ($r_s = 0.722$, $p < 0.001$). The distributions of the UST mean sound speed and MPD were similar in shape and the associations with age and weight were similar. These results minimize the uncertainty in breast density measurements made on a symptomatic population that was present in the previous work.

They also confirm the previously offered conclusions that UST is capable of safely producing consistent measurements of breast density that correlate with MPD, the metric which is best established as a measure of breast cancer risk.

From the results listed in Table 1, the UST mean sound speed (1450.2 m/s) is seen to be higher than both the median (1446.0 m/s) and modal (1440.0 m/s) sound speed. This suggests that for an average participant in our study population, there is a positively skewed distribution of sound speed with the majority of the sound speed values concentrated on low sound speeds with a tail stretching to higher sound speed values. Inspection of the distribution of the mean, median and modal sound speeds throughout the participant population (Figure 2) shows that the mean sound speed is peaked at a higher value than the median and modal sound speed. This observation once again points to the skewness of the individual participants sound speed distributions.

Previous work (Duric, et al. 2013, Duric, et al. 2007, Sak 2013) involving UST density measurements have used the mean sound speed as a measure of breast density. The results from Table 2 suggest that the median sound speed value is comparable to the mean sound speed as a measure of average breast density. Correlations with MPD and most of the subregion measurements are of a similar strength when using the median sound speed instead of the mean sound speed. Manual segmentation of the breast from the water bath is imperfect and on some slices, a small number of voxels that correspond to the water bath are not removed. The sound speed of the water bath is higher than most breast tissue, so these voxels may skew the mean sound speed to a slightly higher value. The median value is less sensitive to these higher sound speed voxels than the mean value and may theoretically be a slightly better measure. However, the advantages of using the median value are small as the mean value does provide correlations with a similar strength. Further study of this relationship is needed.

In Table 1, the average modal sound speed of the group is very similar to the mean sound speed of the non-dense tissue using either segmentation method. Also, the correlations in Table 2 and Table 4 involving the modal sound speed are relatively similar to those involving the sound speed of the non-dense tissue. The modal sound speed value is the most common sound speed value. For the population studied here, the segmented non-dense tissue is more common than segmented dense tissue as the average breast density is low relative to the general population(Sprague, et al. 2014). Therefore, the mean sound speed of the non-dense tissue is likely very similar to the modal value of the entire breast. For fatty breasts, the modal sound speed can be used as an approximation of the sound speed of the non-dense tissue without requiring the use of segmentation of the UST sound speed images.

This study enabled a direct comparison of breast anatomy and the corresponding breast subregions (dense and non-dense tissue) in a 2D mammographic form versus a 3D UST form. The segmentation of the UST sound speed images using the methods described here created volumes of dense and non-dense tissue, which should strongly correlate with the corresponding mammographic areas. For the MPD, which is an area measure, the correlations with the mean and median sound speed values ($r_s = 0.722$, $p < 0.001$ and $r_s = 0.737$, $p < 0.001$) were stronger than with the corresponding k-means USTPD measures ($r_s =$

0.568, $p < 0.001$) but similar to the correlation with threshold USTPD ($r_s = 0.715$, $p < 0.001$). Although the mean and median sound speed values are volumetric measurements that do not have a corresponding mammographic density measure, they still appeared to be a strong measure of average breast density.

Results from the direct comparisons of the UST created dense and non-dense volumes with the mammographic dense and non-dense areas are mixed. It is known that mammographic dense and non-dense area relates to MPD and breast cancer risk (Bertrand, et al. 2015, Pettersson, et al. 2011). The results in Table 2 show moderate to strong associations between the dense and non-dense mammographic area with the average breast density measures of UST mean, median and modal sound speed and with MPD (ranging from $r_s = 0.544$, $p < 0.001$ to $r_s = 0.840$, $p < 0.001$ for dense area and $r_s = -0.499$, $p < 0.001$ to $-0.757$, $p < 0.001$ for non-dense area). However, there are no statistically significant associations between the k-means dense volume and the average density measures ($r_s = -0.014$, $p = 0.863$ to $r_s = -0.116$, $p = 0.137$) and only weak to moderate associations involving the threshold dense volume ($r_s = 0.233$, $p = 0.003$ to $r_s = 0.439$, $p < 0.001$).

As shown in Table 5, the UST dense volumes show a weak yet statistically significant correlation with mammographic dense area ($r_s = 0.198$, $p = 0.011$ for k-means and $r_s = 0.466$, $p < 0.001$ for threshold). The associations of the non-dense and total breast volumes with the non-dense and total breast area are much stronger (ranging from $r_s = 0.745$, $p < 0.001$ to $r_s = 0.780$, $p < 0.001$). Since the study population had relatively low breast density, small variations in the output of the segmentation algorithms had larger effects on the associations involving the dense regions relative to the non-dense regions.

Breast density has typically been defined in a binary fashion as the relative amount of dense and non-dense tissue in the breast. Therefore, the methods used to segment the breast into the dense and non-dense subregions are critical in order to accurately define the internal breast anatomy and discover their relationship with breast cancer risk. Results presented here suggest that relative to mammography, the segmentation methods made using UST do not appear to be as effective at separating dense from non-dense tissue. Therefore, further study of how to properly define subregions in UST sound speed images is still required.

No matter what methods are used to segment the breast, the dense and non-dense regions are treated as homogenous parts of the breast anatomy from scan to scan. Although recent changes to the BIRADS breast composition categories have begun to address the relative density of the dense breast tissue (Sickles, et al. 2013, Slanetz, et al. 2015), the characterization of density when using mammography still uses this binary model and is therefore highly subjective. The additional quantitative information stored in the UST images can provide useful information regarding the relative density of these subregions that mammography cannot.

Using the quantitative nature of the UST sound speed measurements, the dense and non-dense regions were analyzed by measuring the mean sound speed values of the subregions. As expected, the dense subregions show higher sound speed than the non-dense regions. By comparing the standard deviations of the subregion sound speed values, the dense

subregions also have a wider range of possible sound speed values relative to the non-dense regions. Furthermore, the k-means method shows a wider range of possible values than the threshold method. By definition, the threshold method will produce a cap on the possible values the subregion sound speed can have, with the non-dense region having a mean value below 1460 m/s and the dense region having a mean value above 1460 m/s. The k-means method does not have this limitation and therefore the range of possible values is much larger. For the k-means method, the minumum dense subregion sound speed measured was 1451 m/s and the maximum non-dense subregion sound speed measured was 1505 m/s. This indicates that when using the k-means method, some participants with very dense breasts have non-dense regions that are of greater density than the dense regions in women with very fatty breasts. However, the clinical importance of these differences is still unknown.

Irrespective of the method used to define the subregions, the sound speed of the subregions showed correlations with the UST and mammographic average breast density measures. Both the non-dense and dense sound speed show moderate to strong positive correlations with the average UST breast density measures and MPD measurements. Correlations with UST measurements are stronger than those with MPD and the correlations with the non-dense subregion sound speed are stronger than those with the dense sound speed. These results further indicate that dense and non-dense tissues are not uniform across participants.

The participant factors examined here are known to have an effect on both breast cancer risk and breast density. The results from Table 5 show that participant height has no statistically significant relationship with any UST or mammographic density measure. Participant age shows inverse and weak relationships with the density measures. Participant weight and BMI show stronger and positive correlations relative to those with age.

The average BMI of the studied group is 31.2 $kg/m^2$ which is greater than that of the average adult woman in the USA (Flegal, et al. 2012) of 28.7 $kg/m^2$. This increased BMI also likely explains why the breast density for this group skews low with only a few participants with high breast density. Increased weight and BMI are also strongly associated with increased non-dense tissue (Schetter, et al. 2014). This increased non-dense tissue tends to lead to increased total volume and total projected breast area. Given that women with high BMI have more fat tissue in the breast on average and that MPD reflects the relative amounts of dense and non-dense tissue in the breast, it is perhaps expected that correlations between MPD and BMI are stronger than those between BMI and the UST sound speed measurements. The UST sound speed measurements are direct measurements of the breast tissue properties and therefore are less strongly related to the relative amounts of fatty and non-fatty breast tissue than MPD.

Mammography is a tool whose primary use is in the detection of cancer. Measurement of breast density is a secondary use of mammography. Therefore many of the techniques used to aid in detection can introduce uncertainty into mammographic breast density measurements (Yaffe 2008). Compression of the breast is applied to reduce the amount of radiation used and to improve image quality but can be variable between scans, even for the same patient, due to perceived discomfort. Compressed breast tissue in either CC or MLO projection also has inherent differences when transitioning from 2-D area assessments to 3-

D volumetric assessments. There is also some discussion that without additional mammographic imaging characteristics that are not commonly considered when density measurements are made, an accurate volume of dense tissue cannot properly be determined in mammography (Kopans 2008).

It may therefore seem that the physiological differences in breast density may be difficult to distinguish from the technical variabilities of mammography. However, no matter how mammographic density was measured, it has been consistently shown that women with higher breast densities have an increased risk of developing breast cancer. This was true when mammographic density was measured qualitatively using visual estimations of breast density (Saftlas, et al. 1991), quantitatively using area-based measurements (Boyd, et al. 1995) or even using volumetric measures (Ciatto, et al. 2012, Jeffreys, et al. 2010) which more directly incorporate the uncertainties of breast compression. Therefore, despite the concerns regarding the distribution of dense tissue throughout the breast, mammographic density is a robust measurement that is currently well accepted in a wide variety of forms.

UST imaging shares a similar geometry to breast MRI as for both of these modalities, the patient lays face down with their uncompressed breast free-hanging. Previous studies have shown strong correlations of a similar strength to those reported here between volumetric MRI density measures and mammographic breast density measures (Khazen, et al. 2008, Thompson, et al. 2009). While not directly compared here in this work, these other results suggest that breast MRI and UST imaging likely handle the technical variabilities introduced by mammography in a similar fashion.

Finally, this work was meant to compare how the two unique imaging modalites of UST and mammography represent dense tissue. UST sound speed imaging is a novel imaging modality and gives a more direct representation of the tissue density than mammography does. These unique properties of UST sound speed imaging may ultimately overcome the limitations present in mammography in regards to the measurement of breast density. This work therefore lays the groundwork for further studies that will assess the role of sound speed imaging in risk prediction.

## Conclusion

In this group of women with negative mammographic screens (N=165), various volumetric breast density measurements made using UST were found to correlate strongly with 2D breast density measurements made with mammography. The results presented here validate previous work done involving UST sound speed measures in symptomatic populations. These results reduce the uncertainties that were present in the previous work regarding breast density measurements and increases the confidence in the ability of UST to accurately measure breast density in a wide range of participants.

The mean and median sound speed values showed stronger correlations with MPD than UST percent density measures. The amount of dense tissue, whether measured using projected areas on a mammogram or volumetrically using one of two different methods on the UST sound speed images was positively associated with the average UST and mammographic density measures. Although the segmention methods used to create dense and non-dense

volumes could still be improved, initial analysis of the dense and non-dense subregions using UST sound speed provides evidence that breast density is more than just the relative amounts of these tissues as visualized on an image. The relative density of these regions can vary as the average density of the entire breast varies, although it is currently unkown whether this provides additional breast cancer risk information. Mammography and UST also show similar behaviour when associated with participant age, weight and BMI.

UST is a useful tool that can be used to analyze breast density in ways that mammography cannot. These results suggest that UST and mammography provide different information about breast tissue composition. UST sound speed measurements have not been evaluated prospectively to estimate risk of developing breast cancer. However, given that UST breast density measures and MPD correlate strongly, it is expected that UST density measures will also be strong breast cancer risk factors. Future studies are needed to compare UST and MPD in risk prediction.

## Acknowledgments

The authors wish to thank Dr. Norman Boyd for his work analyzing all mammograms and Ms. Vivian Linke for research assistance. The authors are indebted to the participants in the Ultrasound Study of Tamoxifen for their outstanding cooperation and to the physicians, pathologists, nurses and technologists for their efforts in the field.

**Funding**

This research was supported in part by the Intramural Research Program of the National Institutes of Health, National Cancer Institute. The authors acknowledge the support of the National Institutes of Health through contract No HHSN261201400038P and grant No R44CA165320 from the National Cancer Institute.

## References

Bertrand KA, Scott CG, Tamimi RM, Jensen MR, Pankratz VS, Norman AD, Visscher DW, Couch FJ, Shepherd J, Chen Y-Y, Fan B, Wu F-F, Ma L, Beck AH, Cummings SR, Kerlikowske K, Vachon CM. Dense and Nondense Mammographic Area and Risk of Breast Cancer by Age and Tumor Characteristics. Cancer Epidemiology Biomarkers & Prevention. 2015; 24:798–809.

Boyd NF, Byng JW, Jong RA, Fishell EK, Little LE, Miller AB, Lockwood GA, Tritchler DL, Yaffe MJ. Quantitative Classification of Mammographic Densities and Breast Cancer Risk: Results From the Canadian National Breast Screening Study. Journal of the National Cancer Institute. 1995; 87:670–75. [PubMed: 7752271]

Byng JW, Boyd NF, Fishell E, Jong RA, Yaffe MJ. The quantitative analysis of mammographic densities. Physics in Medicine and Biology. 1994; 39:1629. [PubMed: 15551535]

Byrne C, Schairer C, Wolfe J, Parekh N, Salane M, Brinton LA, Hoover R, Haile R. Mammographic Features and Breast Cancer Risk: Effects With Time, Age, and Menopause Status. Journal of the National Cancer Institute. 1995; 87:1622–29. [PubMed: 7563205]

Ciatto S, Bernardi D, Calabrese M, Durando M, Gentilini MA, Mariscotti G, Monetti F, Moriconi E, Pesce B, Roselli A, Stevanin C, Tapparelli M, Houssami N. A first evaluation of breast radiological density assessment by QUANTRA software as compared to visual classification. The Breast. 2012; 21:503–06. [PubMed: 22285387]

Duric N, Boyd N, Littrup P, Sak M, Myc L, Li C, West E, Minkin S, Martin L, Yaffe M, Schmidt S, Faiz M, Shen J, Melnichouk O, Li Q, Albrecht T. Breast density measurements with ultrasound tomography: A comparison with film and digital mammography. Medical Physics. 2013; 40:013501–12. [PubMed: 23298122]

Duric N, Littrup P, Babkin A, Chambers D, Azevedo S, Kalinin A, Pevzner R, Tokarev M, Holsapple E, Rama O, Duncan R. Development of ultrasound tomography for breast imaging: Technical assessment. Medical Physics. 2005; 32:1375–86. [PubMed: 15984689]

Duric N, Littrup P, Chandiwala-Mody P, Li C, Schmidt S, Myc L, Rama O, Bey-Knight L, Lupinacci J, Ranger B, Szczepanski A, West E. In-vivo imaging results with ultrasound tomography: report on an ongoing study at the Karmanos Cancer Institute. Medical Imaging 2010: Ultrasonic Imaging, Tomography, and Therapy. 2010:76290M. Proc. SPIE7629.

Duric N, Littrup P, Li C, Rama O, Bey-Knight L, Schmidt S, Lupinacci J. Detection and characterization of breast masses with ultrasound tomography: clinical results. Medical Imaging 2009: Ultrasonic Imaging and Signal Processing. 2009:72651G. Proc. SPIE7265.

Duric N, Littrup P, Poulo L, Babkin A, Pevzner R, Holsapple E, Rama O, Glide C. Detection of breast cancer with ultrasound tomography: First results with the Computed Ultrasound Risk Evaluation (CURE) prototype. Medical Physics. 2007; 34:773–85. [PubMed: 17388195]

Duric N, Littrup P, Schmidt S, Li C, Roy O, Bey-Knight L, Janer R, Kunz D, Chen X, Goll J, Wallen A, Zafar F, Allada V, West E, Jovanovic I, Li K, Greenway W. Breast Imaging with the SoftVue Imaging system: First results. Medical Imaging 2013: Ultrasonic Imaging, Tomography, and Therapy. 2013:8675–19. Proc. SPIE8675.

Eng A, Gallant Z, Shepherd J, McCormack V, Li J, Dowsett M, Vinnicombe S, Allen S, dos-Santos-Silva I. Digital mammographic density and breast cancer risk: a case-control study of six alternative density assessment methods. Breast Cancer Res. 2014; 16:439. [PubMed: 25239205]

Flegal KM, Carroll MD, Kit BK, Ogden CL. Prevalence of obesity and trends in the distribution of body mass index among us adults, 1999–2010. JAMA. 2012; 307:491–97. [PubMed: 22253363]

Huo CW, Chew GL, Britt KL, Ingman WV, Henderson MA, Hopper JL, Thompson EW. Mammographic density—a review on the current understanding of its association with breast cancer. Breast Cancer Research and Treatment. 2014; 144:479–502. [PubMed: 24615497]

Jain, AK., Dubes, RC. Algorithms for clustering data. Prentice-Hall, Inc.; 1988.

Jeffreys, M., Harvey, J., Highnam, R. Comparing a New Volumetric Breast Density Method (VolparaTM) to Cumulus. In: Martí, J.Oliver, A.Freixenet, J., Martí, R., editors. Digital Mammography. Springer; Berlin Heidelberg: 2010. p. 408-13.

Khazen M, Warren RML, Boggis CRM, Bryant EC, Reed S, Warsi I, Pointon LJ, Kwan-Lim GE, Thompson D, Eeles R, Easton D, Evans DG, Leach MO. A Pilot Study of Compositional Analysis of the Breast and Estimation of Breast Mammographic Density Using Three-Dimensional T1-Weighted Magnetic Resonance Imaging. Cancer Epidemiology Biomarkers & Prevention. 2008; 17:2268–74.

Khodr ZG, Sak MA, Pfeiffer RM, Duric N, Littrup P, Bey-Knight L, Ali H, Vallieres P, Sherman ME, Gierach GL. Determinants of the reliability of ultrasound tomography sound speed estimates as a surrogate for volumetric breast density. Medical Physics. 2015; 42:5671–78. [PubMed: 26429241]

Kopans DB. Basic Physics and Doubts about Relationship between Mammographically Determined Tissue Density and Breast Cancer Risk1. Radiology. 2008; 246:348–53. [PubMed: 18227535]

Li C, Duric N, Huang L. Clinical breast imaging using sound-speed reconstructions of ultrasound tomography data. Medical Imaging 2008: Ultrasonic Imaging and Signal Processing. 2008:692009. Proc. SPIE6920.

Mast TD. Empirical relationships between acoustic parameters in human soft tissues. Acoustics Research Letters Online. 2000; 1:37–42.

Masugata H, Mizushige K, Senda S, Kinoshita A, Sakamoto H, Sakamoto S, Matsuo H. Relationship between myocardial tissue density measured by microgravimetry and sound speed measured by acoustic microscopy. Ultrasound in Medicine & Biology. 1999; 25:1459–63. [PubMed: 10626635]

McCormack VA, dos Santos Silva I. Breast Density and Parenchymal Patterns as Markers of Breast Cancer Risk: A Meta-analysis. Cancer Epidemiology Biomarkers & Prevention. 2006; 15:1159–69.

Pettersson A, Graff RE, Ursin G, Santos Silva Id, McCormack V, Baglietto L, Vachon C, Bakker MF, Giles GG, Chia KS, Czene K, Eriksson L, Hall P, Hartman M, Warren RML, Hislop G, Chiarelli AM, Hopper JL, Krishnan K, Li J, Li Q, Pagano I, Rosner BA, Wong CS, Scott C, Stone J, Maskarinec G, Boyd NF, van Gils CH, Tamimi RM. Mammographic Density Phenotypes and Risk of Breast Cancer: A Meta-analysis. Journal of the National Cancer Institute. 2014

Pettersson A, Hankinson SE, Willett WC, Lagiou P, Trichopoulos D, Tamimi RM. Nondense mammographic area and risk of breast cancer. Breast Cancer Res. 2011; 13:R100. [PubMed: 22017857]

Rasband, WS. ImageJ. Bethesda, Maryland, USA: US National Institutes of Health; 1997–2012.

Regini E, Mariscotti G, Durando M, Ghione G, Luparia A, Campanino P, Bianchi C, Bergamasco L, Fonio P, Gandini G. Radiological assessment of breast density by visual classification (BI–RADS) compared to automated volumetric digital software (Quantra): implications for clinical practice. Radiol med. 2014:1–9. [PubMed: 24263456]

Saftlas AF, Hoover RN, Brinton LA, Szklo M, Olson DR, Salane M, Wolfe JN. Mammographic densities and risk of breast cancer. Cancer. 1991; 67:2833–38. [PubMed: 2025849]

Sak M, Duric N, Boyd N, Littrup P, West E, Li C. Breast tissue composition and breast density measurements from ultrasound tomography. Medical Imaging 2012: Ultrasonic Imaging, Tomography, and Therapy. 2012:83200Q. Proc. SPIE8320.

Sak M, Duric N, Boyd NF, Littrup P, Myc L, Faiz M, Li C, Bey-Knight L. Relationship between breast sound speed and mammographic percent density. Medical Imaging 2011: Ultrasonic Imaging, Tomography, and Therapy. 2011:7968. Proc. SPIE7968.

Sak M, Duric N, Littrup P, Bey-Knight L, Sherman M, Gierach G, Malyarenko A. Comparison of sound speed measurements on two different ultrasound tomography devices. Medical Imaging 2014: Ultrasonic Imaging, Tomography, and Therapy. 2014:9040. Proc. SPIE9040.

Sak M, Duric N, Littrup P, Li C, Bey-Knight L, Sherman M, Boyd NF, Gierach G. Breast density measurements using ultrasound tomography for patients undergoing tamoxifen treatment. Medical Imaging 2013: Ultrasonic Imaging, Tomography, and Therapy. 2013:8675. Proc. SPIE8675.

Sak, MA. The role of tissue sound speed as a surrogate marker of breast density. Ann Arbor: Wayne State University; 2013. p. 225

Sak MA, Littrup PJ, Duric N, Mullooly M, Sherman ME, Gierach GL. Current and future methods for measuring breast density: a brief comparative review. Breast Cancer Management. 2015:4.

Schetter S, Hartman T, Liao J, Richie J, Prokopczyk B, DuBrock C, Signori C, Hamilton C, Demers L, El-Bayoumy K, Manni A. Differential impact of body mass index on absolute and percent breast density: implications regarding their use as breast cancer risk biomarkers. Breast Cancer Research and Treatment. 2014; 146:355–63. [PubMed: 24951269]

Sickles, EA., D'Orsi, CJ., Bassett, LW. ACR BI-RADS® Mammography. Reston, VA: American College of Radiology; 2013.

Slanetz PJ, Freer PE, Birdwell RL. Breast-Density Legislation — Practical Considerations. New England Journal of Medicine. 2015; 372:593–95. [PubMed: 25671249]

Sprague BL, Gangnon RE, Burt V, Trentham-Dietz A, Hampton JM, Wellman RD, Kerlikowske K, Miglioretti DL. Prevalence of Mammographically Dense Breasts in the United States. Journal of the National Cancer Institute. 2014:106. [PubMed: 25174031]

Thompson DJ, Leach MO, Kwan-Lim G, Gayther SA, Ramus SJ, Warsi I, Lennard F, Khazen M, Bryant E, Reed S. Assessing the usefulness of a novel MRI-based breast density estimation algorithm in a cohort of women at high genetic risk of breast cancer: the UK MARIBS study. Breast Cancer Res. 2009; 11:R80. [PubMed: 19903338]

Weiwad W, Heinig A, Goetz L, Hartmann H, Lampe D, Buchmann J, Millner R, Spielmann RP, Heywang-Koebrunner SH. Direct Measurement of Sound Velocity in Various Specimens of Breast Tissue. Investigative Radiology. 2000; 35:721–26. [PubMed: 11204798]

Yaffe MJ. Mammographic density. Measurement of mammographic density. Breast Cancer Research. 2008; 10:1–10.

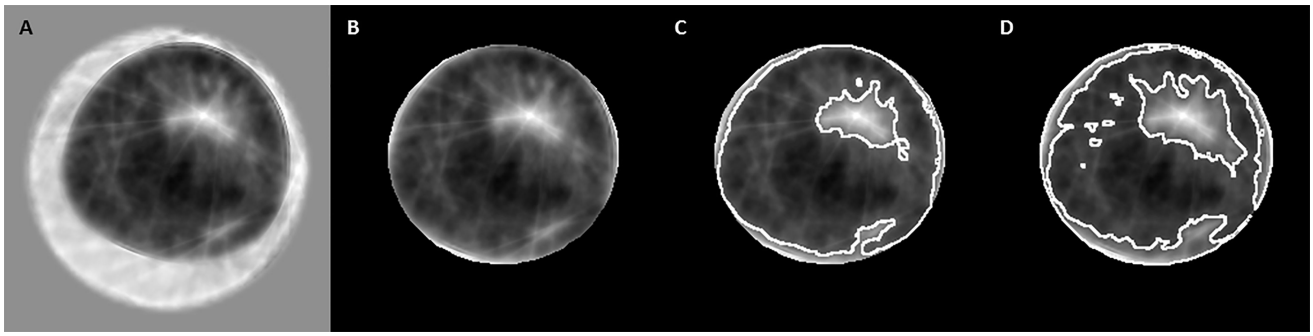


**Figure 1.**

A standard UST sound speed image (A); The same image after it has been masked to separate it from the background water (B); The masked image segmented into dense and non-dense tissue using the k-means clustering method (C); The masked image segmented into dense and non-dense tissue using the threshold method (D).

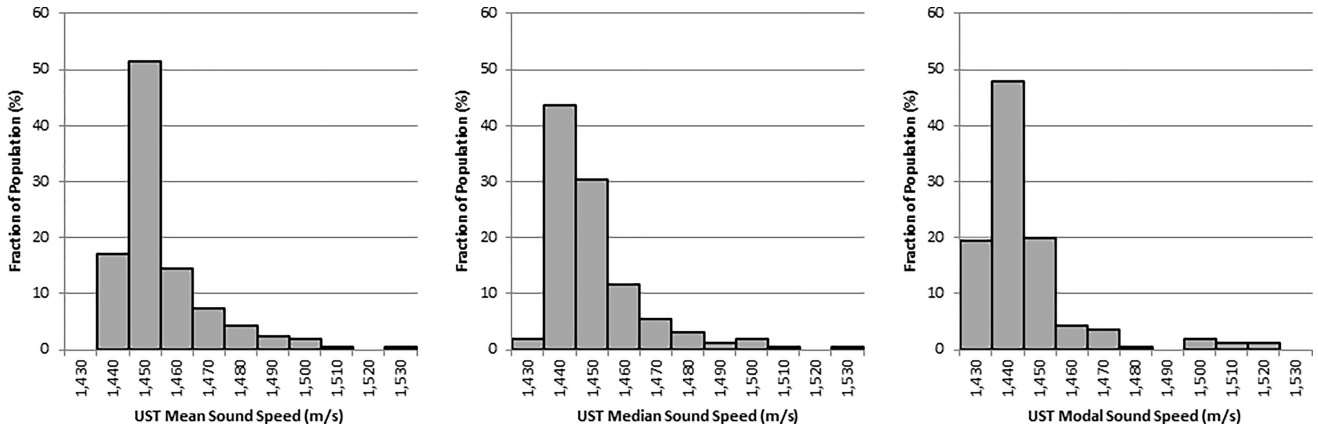


**Figure 2.**

Participant frequency distributions of the Ultrasound tomography (UST) Mean (Left), Median (Middle) and Modal (Right) sound speed.

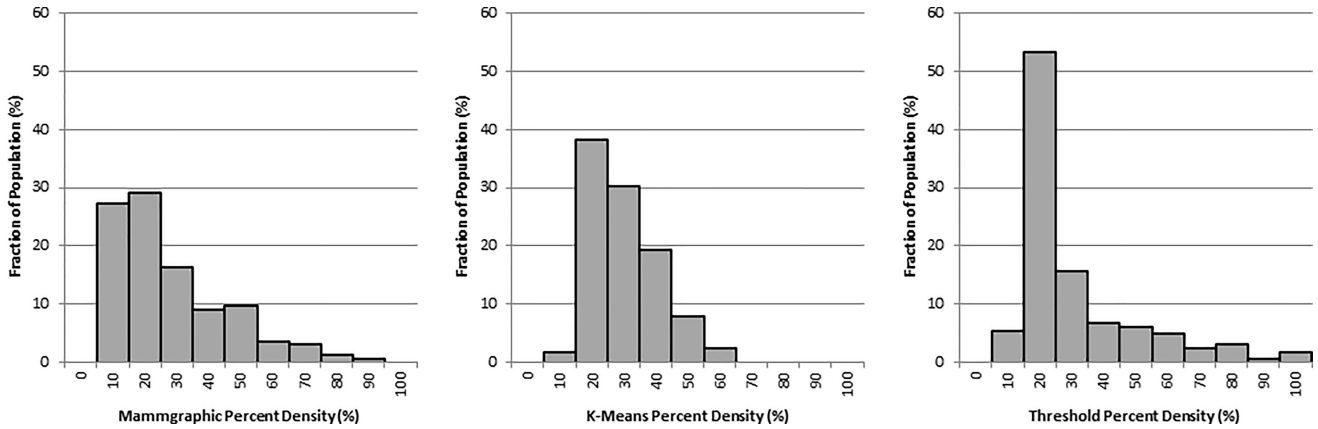


**Figure 3.**

Participant distributions of the mammographic percent density (Left) along with the Ultrasound tomography (UST) K-Means percent density (middle) and UST threshold percent density (Right).

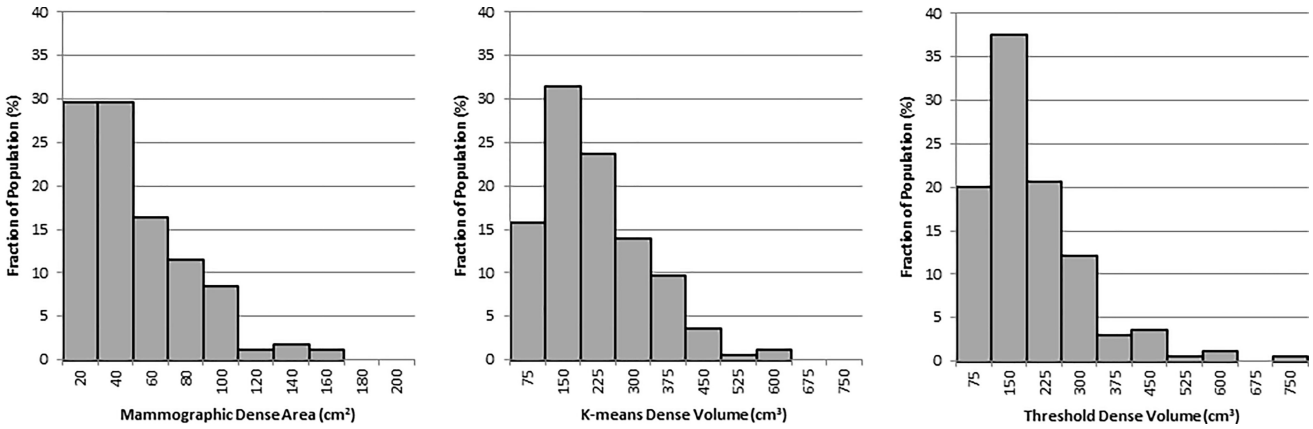


**Figure 4.**

Participant distributions of the projected mammographic dense area (Left), Ultrasound tomography (UST) k-means dense volume (middle) and UST threshold dense volume (Right).

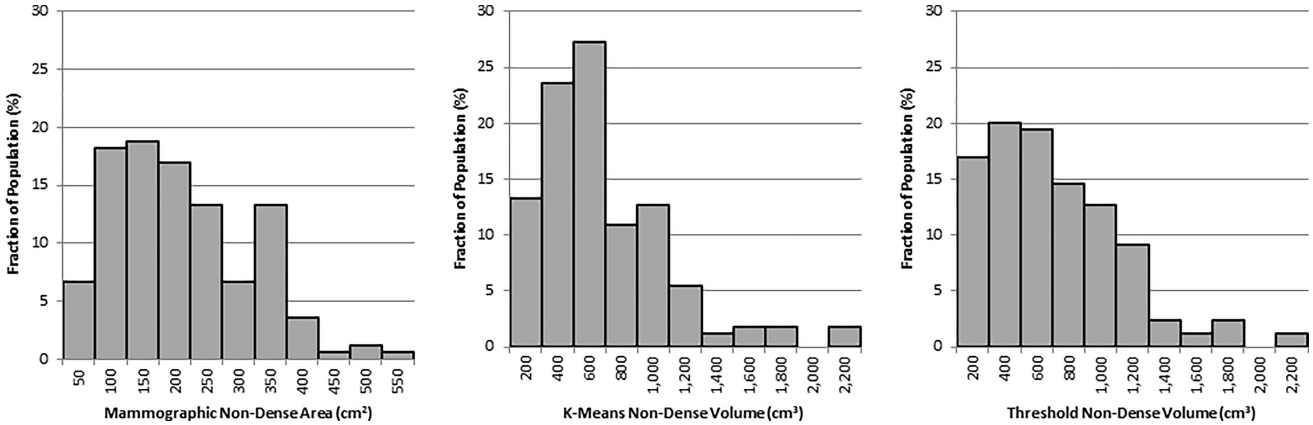


**Figure 5.**

Participant distributions of the projected mammographic non-dense area (Left), Ultrasound tomography (UST) k-means non-dense volume (Middle) and UST threshold non-dense volume (Right).

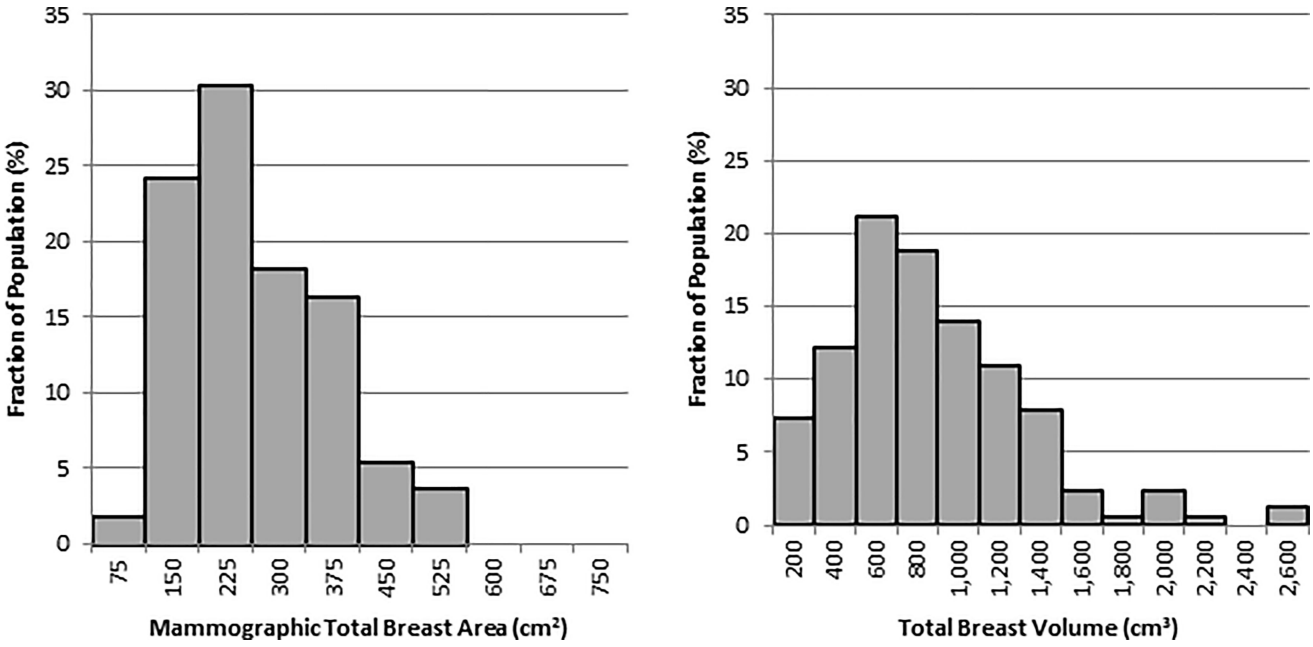


**Figure 6.**

Participant distributions of the total projected mammographic breast area (Left) and the Ultrasound tomography (UST) total breast volume (Right).

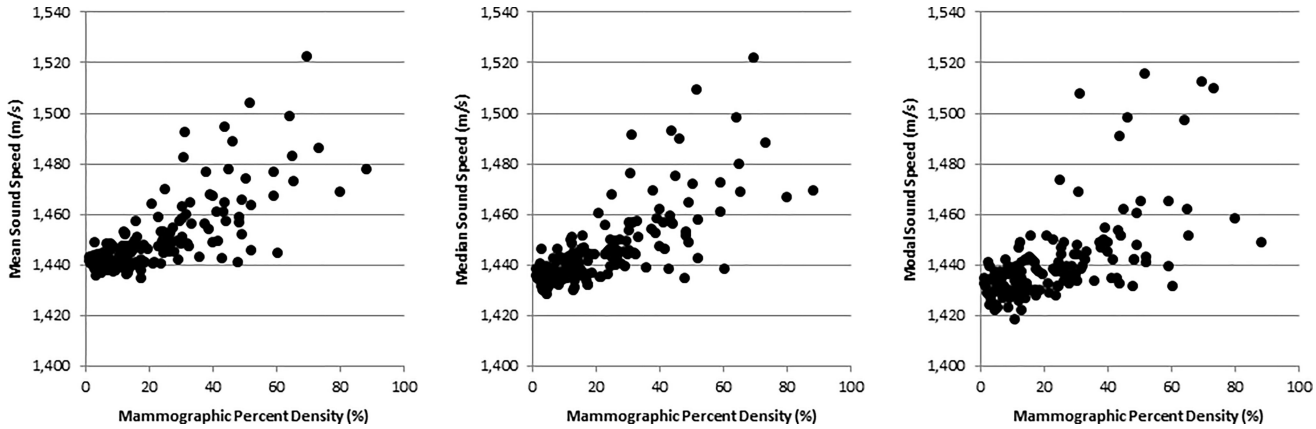


**Figure 7.**

Plots of the Ultrasound tomography (UST) Mean (Left), Median (Middle) and Modal (Right) sound speed versus the mammographic percent density.

## Table 1

Average Values for Various Imaging and Participant Characteristics (N = 165)

| | Average Value (SD) |
|---|---|
| **UST Sound Speed Image Characteristics** | |
| UST Mean Sound Speed (m/s) | 1450.2 (14.5) |
| UST Median Sound Speed (m/s) | 1446.0 (15.4) |
| UST Modal Sound Speed (m/s) | 1440.0 (16.7) |
| UST Total Volume ($cm^3$) | 777.5 (478.6) |
| **Mammographic Image Characteristics** | |
| Mammographic Percent Density (%) | 22.4 (18.0) |
| Mammographic Dense Projected Area ($cm^2$) | 41.9 (31.4) |
| Mammographic Non-Dense Projected Area ($cm^2$) | 185.1 (105.0) |
| Mammographic Total Projected Area ($cm^2$) | 227.0 (102.7) |
| **UST K-Means Clustering Subregion Characteristics** | |
| K-Means Mean Dense Sound Speed (m/s) | 1480.1 (16.5) |
| K-Means Mean Non-Dense Sound Speed (m/s) | 1439.9 (10.8) |
| K-Means Dense Volume ($cm^3$) | 180.1 (110.4) |
| K-Means Non-Dense Volume ($cm^3$) | 592.9 (405.8) |
| K-Means Percent Density (%) | 25.3 (10.5) |
| **UST Threshold Subregion Characteristics** | |
| Threshold Mean Dense Sound Speed (m/s) | 1481.1 (7.5) |
| Threshold Mean Non-Dense Sound Speed (m/s) | 1438.6 (5.1) |
| Threshold Dense Volume ($cm^3$) | 163.6 (125.3) |
| Threshold Non-Dense Volume ($cm^3$) | 609.5 (427.7) |
| Threshold Percent Density (%) | 25.5 (19.7) |
| **Participant Characteristics** | |
| Participant Age (years) | 51.4 (8.0) |
| Participant Height (inches) | 64.4 (3.3) |
| Participant Weight (pounds) | 184.0 (45.6) |
| Participant BMI ($kg/m^2$) | 31.2 (7.7) |
| Time Between Mammogram and UST Scan (days) | 42 (23) |

## Table 2

Correlations of Average Density Measures and Subregion Density Measures for UST and Mammography

| | UST Mean Sound Speed (km/s) | UST Median Sound Speed (km/s) | UST Modal Sound Speed (km/s) | Mammographic Percent Density |
|---|---|---|---|---|
| **UST Median Sound Speed (km/s)** | 0.984 | | | |
| **UST Modal Sound Speed (km/s)** | 0.883 | 0.913 | | |
| **Mammographic Percent Density** | 0.722 | 0.737 | 0.651 | |
| **K-Means Mean Dense Sound Speed (m/s)** | 0.688 | 0.633 | 0.577 | 0.451 |
| **K-Means Mean Non-Dense Sound Speed (m/s)** | 0.915 | 0.908 | 0.866 | 0.612 |
| **K-Means Dense Volume ($cm^3$)** | −0.014 (0.863) | −0.029 (0.715) | −0.116 (0.137) | −0.099 (0.207) |
| **K-Means Non-Dense Volume ($cm^3$)** | −0.464 | −0.492 | −0.473 | −0.526 |
| **K-Means Percent Density (%)** | 0.572 | 0.592 | 0.454 | 0.568 |
| **Threshold Mean Dense Sound Speed (m/s)** | 0.411 | 0.340 | 0.264 | 0.295 |
| **Threshold Mean Non-Dense Sound Speed (m/s)** | 0.813 | 0.831 | 0.817 | 0.545 |
| **Threshold Dense Volume ($cm^3$)** | 0.439 | 0.390 | 0.278 | 0.233 (0.003) |
| **Threshold Non-Dense Volume ($cm^3$)** | −0.549 | −0.566 | −0.539 | −0.580 |
| **Threshold Percent Density (%)** | 0.929 | 0.885 | 0.754 | 0.715 |
| **UST Total Volume ($cm^3$)** | −0.371 | −0.395 | −0.401 | −0.447 |
| **Mammographic Total Breast Area ($cm^2$)** | −0.378 | −0.402 | −0.359 | −0.557 |
| **Mammographic Dense Area ($cm^2$)** | 0.614 | 0.624 | 0.544 | 0.850 |
| **Mammographic Non-Dense Area ($cm^2$)** | −0.539 | −0.561 | −0.499 | −0.757 |

Each cell contains Spearman correlation coefficient with p-value shown in brackets. For entries without bracket, p-value was $p < 0.001$. Blank entries correspond to redundant correlations or correlations of the same density value.

**Table 3**

Correlations of Subregion Density Measures Made by Both Segmentation Methods

| | K-Means Dense Sound Speed (m/s) | K-Means Non-Dense Sound Speed (km/s) | K-Means Dense Volume ($cm^3$) | K-Means Non-Dense Volume ($cm^3$) | K-Means Percent Density | Total Breast Volume ($cm^3$) |
|---|---|---|---|---|---|---|
| **Threshold Dense Sound Speed (m/s)** | 0.788 | 0.323 | −0.024 (0.762) | −0.161 (0.039) | 0.159 (0.041) | −0.126 (0.106) |
| **Threshold Non-Dense Sound Speed (m/s)** | 0.394 | 0.869 | 0.021 (0.786) | −0.308 | 0.419 | −0.238 (0.002) |
| **Threshold Dense Volume ($cm^3$)** | 0.440 | 0.400 | 0.743 | 0.432 | 0.219 (0.005) | 0.547 |
| **Threshold Non-Dense Volume ($cm^3$)** | −0.363 | −0.441 | 0.634 | 0.972 | −0.508 | 0.956 |
| **Threshold Percent Density** | 0.690 | 0.762 | −0.001 (0.991) | −0.494 | 0.637 | −0.398 |
| **Total Breast Volume ($cm^3$)** | −0.205 (0.008) | −0.290 | 0.781 | 0.970 | −0.366 | N/A |

Each cell contains Spearman correlation coefficient with p-value shown in brackets. For entries without bracket, p-value was $p < 0.001$.

## Table 4

Correlations of Mammographic Subregion Density Measures with UST Density Measures

| | Mammographic Dense Area ($cm^2$) | Mammographic Non-Dense Area ($cm^2$) | Total Mammographic Breast Area ($cm^2$) |
|---|---|---|---|
| **K-Means Mean Dense Sound Speed (m/s)** | 0.367 | −0.323 | −0.194 (0.012) |
| **K-Means Mean Non-Dense Sound Speed (m/s)** | 0.584 | −0.381 | −0.212 (0.006) |
| **K-Means Dense Volume ($cm^3$)** | 0.198 (0.011) | 0.408 | 0.501 |
| **K-Means Non-Dense Volume ($cm^3$)** | −0.168 (0.031) | 0.764 | 0.764 |
| **K-Means Percent Density (%)** | 0.412 | −0.542 | −0.451 |
| **Threshold Mean Dense Sound Speed (m/s)** | 0.178 (0.022) | −0.277 | −0.196 (0.012) |
| **Threshold Mean Non-Dense Sound Speed (m/s)** | 0.579 | −0.292 | −0.135 (0.084) |
| **Threshold Dense Volume ($cm^3$)** | 0.466 | 0.153 (0.050) | 0.326 |
| **Threshold Non-Dense Volume ($cm^3$)** | −0.233 | 0.780 | 0.748 |
| **Threshold Percent Density (%)** | 0.569 | −0.577 | −0.428 |
| **Total Breast Volume ($cm^3$)** | −0.082 (0.296) | 0.720 | 0.745 |

Each cell contains Spearman correlation coefficient with p-value shown in brackets. For entries without bracket, p-value was $p < 0.001$.

## Table 5

UST and Mammographic Density Correlations with Participant Characteristics

| | Age (years) | Height (inches) | Weight (pounds) | BMI (kg/m$^2$) |
|---|---|---|---|---|
| **UST Sound Speed Image Characteristics** | | | | |
| UST Mean Sound Speed (m/s) | −0.239 (0.002) | 0.118 (0.131) | −0.429 | −0.429 |
| UST Median Sound Speed (m/s) | −0.226 (0.004) | 0.114 (0.144) | −0.447 | −0.447 |
| UST Modal Sound Speed (m/s) | −0.114 (0.144) | 0.061 (0.433) | −0.417 | −0.409 |
| UST Total Volume (cm$^3$) | −0.089 (0.256) | −0.004 (0.955) | 0.499 | 0.513 |
| **Mammographic Image Characteristics** | | | | |
| Mammographic Percent Density (%) | −0.204 (0.008) | 0.105 (0.180) | −0.477 | −0.489 |
| Mammographic Total Projected Area (cm$^2$) | −0.040 (0.611) | 0.021 (0.793) | 0.573 | 0.570 |
| Mammographic Non-Dense Projected Area (cm$^2$) | 0.036 (0.649) | −0.012 (0.882) | 0.600 | 0.599 |
| Mammographic Dense Projected Area (cm$^2$) | −0.262 | 0.122 (0.119) | −0.209 (0.007) | −0.213 (0.006) |
| **UST K-Means Clustering Subregion Characteristics** | | | | |
| K-Means Mean Dense Sound Speed (m/s) | −0.097 (0.213) | 0.080 (0.308) | −0.226 (0.004) | −0.231 (0.003) |
| K-Means Mean Non-Dense Sound Speed (m/s) | −0.160 (0.040) | 0.104 (0.183) | −0.324 | −0.334 |
| K-Means Dense Volume (cm$^3$) | −0.256 | 0.074 (0.344) | 0.233 (0.003) | 0.252 |
| K-Means Non-Dense Volume (cm$^3$) | −0.012 (0.880) | −0.026 (0.742) | 0.548 | 0.557 |
| K-Means Percent Density (%) | −0.247 (0.001) | 0.134 (0.087) | −0.443 | −0.446 |
| **UST Threshold Subregion Characteristics** | | | | |
| Threshold Mean Dense Sound Speed (m/s) | −0.038 (0.387) | 0.097 (0.213) | −0.151 (0.053) | −0.161 (0.039) |
| Threshold Mean Non-Dense Sound Speed (m/s) | −0.155 (0.047) | 0.084 (0.282) | −0.263 | −0.280 |
| Threshold Dense Volume (cm$^3$) | −0.306 | 0.064 (0.412) | 0.0140 (0.854) | 0.045 (0.567) |
| Threshold Non-Dense Volume (cm$^3$) | −0.003 (0.973) | −0.020 (0.777) | 0.552 | 0.557 |
| Threshold Percent Density (%) | −0.224 (0.004) | 0.112 (0.153) | −0.450 | −0.448 |

Each cell contains Spearman correlation coefficient with p-value shown in brackets. For entries without bracket, p-value was $p < 0.001$.